Solid State Ionics 72 (1994) 209–217
North-Holland

SOLID
STATE
IONICS

Structure, microstructure and transport properties of mixed ionic–electronic conductors based on bismuth oxide Part I. Bi–Y–Cu–O system

Yousheng Shen, Ashok Joshi
Ceramatec, Inc., 2425 South 900 West, Salt Lake City, UT 84119, USA

Meilin Liu
School of Materials Engineering, Georgia Institute of Technology, Atlanta, GA 30332, USA

and

Kevin Krist
Gas Research Institute, 8600 West Bryn Mawr Avenue, Chicago, IL 60631, USA

An ionic–electronic mixed conductor consisting of a stabilized fcc $Bi_{1.5}Y_{0.5}O_3$ ionic conductive matrix phase, and a tetragonal $Bi_2Cu_{1-n}^{2+}Cu_n^{1+}O_{4-0.5n}$ electronic conductive second phase has been developed. The ionic transference number and conductivity of the composite material depend critically on the amount of the bismuth copper oxide second phase and its morphology.

1. Introduction

We have already reported that by introducing multivalent titanium oxide into yttria-stabilized bismuth oxide, an ionic–electronic mixed conducting solid solution ($Bi_{1.5}Y_{0.5-x}Ti_xO_{3+0.5x}$) was formed [1,2]. The introduced electronic conduction in such a solid solution is due to the electron hopping through transitions between titanium oxidation states. Another method used to synthesize a mixed conductor is to introduce an electronic conducting second phase into an ionic conductor. Recently, Subramanian et al. [3] reported a two-phase mixed conductor based on a sodium-ion-conducting β-alumina and an electronic-conducting iron oxide. In this paper, we report a newly developed, oxygen-ion and electronic mixed conductive composite material consisting of a $Bi_{1.5}Y_{0.5}O_3$ ionic conducting matrix phase and a $Bi_2CuO_{4-0.5n}$ electronic conducting second phase.

2. Experiments

2.1. Sample preparation

To fabricate the mixed conducting composite materials, the oxides of Bi_2O_3, Y_2O_3 and Cu_2O with the desired ratios according to the formula $(Bi_{1.5}Y_{0.5}O_3)_{(100-x)mol\%}(Bi_2CuO_{4-0.5n})_{xmol\%}$, were mixed and ground. The powder was isostatically pressed into pellets at a pressure of 30000 psi. The green density was 60% of the theoretical density. The samples were sintered in air for 4 h. The theoretical densities were calculated from X-ray diffraction (XRD) data. The densities of sintered pellets were higher than 95% of their theoretical density. Preparation details were described elsewhere [4].

2.2. Crystal structures and microstructures

The crystal structures were identified by XRD at room temperature (Cu Kα). Microstructures were examined by a scanning electron microscope (SEM)

coupled with X-ray mapping. All samples were thermally etched to reverse the grain boundaries.

2.3. Chemical composition

The chemical compositions of the phases were directly analyzed by wavelength dispersion spectroscopy (WDS) microprobe under the image of the SEM. The size of the incident WDS beam was 1 μm or less. The instrument was calibrated using a synthesized $Bi_{1.5}Y_{0.5}O_3$ solid solution material and a copper oxide (CuO). The sensitivity of the instrument is about 0.2 wt % of the absolute concentration.

2.4. Valence state measurement

The valence states of bismuth and copper at temperatures of 25 and 750°C, respectively, were analyzed by an X-ray photoelectron spectroscope (XPS) under a vacuum of 10^{-9} Torr. Al Kα radiation with a 10 eV pass energy was used. The measurement was conducted immediately after sputtering with argon ions on the sample surface to remove any surface contamination. For details of the experimental procedure, see refs. [2,5].

2.5. Electrical conductivity measurement

A two-probe ac complex impedance measurement operating in the frequency domain from 10 MHz to 10 mHz was used to study the temperature and oxygen partial pressure dependences on the electrical conductivity. All samples (15 mm dia. × 5 mm thick) have well-defined cross-sections. For more details on the experimental procedure, see ref. [5].

2.6. Transference number measurement

The oxygen ionic transference number was measured by the electromotive force technique (EMF) according to C. Wanger [6] in an oxygen concentration cell with $P_{O_2} = 0.21$ atm at the cathode and 6×10^{-5} atm at the anode. Details of the experimental procedure are described in ref. [5]. The ionic transference number was calculated according to:

$$t_i = E_{\text{measuring}}/E_{\text{theoretical}} = \sigma_{\text{ionic}}/(\sigma_{\text{ionic}} + \sigma_{\text{electronic}}) . \quad (1)$$

3. Results

3.1. Microstructure

SEM and WDS dot mappings (fig. 1) indicate that the bismuth is distributed in both the matrix phase and the second phase whereas yttrium appears in the matrix phase only, and copper is mainly present in the second phase. As can be seen from the figure, a continuous network second phase is formed around the grain boundaries of the matrix phase.

3.2. Chemical compositions of the phases

Table 1 shows $Bi_{1.5}Y_{0.5}O_3$ chemical compositions for the matrix phase measured by WDS. As can be seen from the table, the data shows that the matrix phase has 0.5 mol% of Cu (x = 0.5 mol% = Cu/(Cu + Y + Bi)). In all cases when the amount of copper in the Bi–Y–Cu–O system varies from one mol% to 50 mol%, the concentration of the copper measured in the matrix phase is always about 0.5 mol%. Table 2 shows a $Bi_2CuO_{(4-0.5n)}$ (n=0.5) chemical compositions for the second phase obtained by WDS.

3.3. Crystal structures

Fig. 2 is a typical XRD pattern of $(Bi_{1.5}Y_{0.5}O_3)_{(100-x)\text{mol}\%}(Bi_2CuO_{4-0.5n})_{x\text{mol}\%}$ where x=15. A set of nine peaks referring to BiY oxide solid solution [7] are clearly shown in all $(Bi_{1.5}Y_{0.5}O_3)_{(100-x)\text{mol}\%}(Bi_2CuO_{4-0.5n})_{x\text{mol}\%}$ materials where x varies from 1 to 50. When $x > 0.03$, there are several small peaks (see fig. 2), representing a tetragonal second phase ($Bi_2CuO_{4-0.5n}$). XRD of the synthesized $Bi_2CuO_{4-0.5n}$ material is plotted in fig. 2.

3.4. Valence states

Fig. 3 shows the spectrum for the binding energy of bismuth ($4f_{7/2}$) in $Bi_{1.5}Y_{0.5}O_3$ and $Bi_2CuO_{4-0.5n}$, respectively and fig. 4 shows the spectrum for the binding energies of copper ($2p_{3/2}$) at 750°C for $(Bi_{1.5}Y_{0.5}O_3)_{(100-x)\text{mol}\%}(Bi_2CuO_{4-0.5n})_{x\text{mol}\%}$ and $Bi_2CuO_{4-0.5n}$. As can been seen from the figure, copper ($2p_{3/2}$) shows two overlapping binding energies.

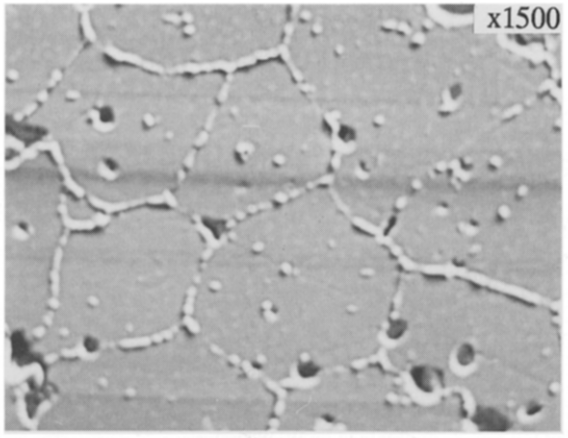

(a)

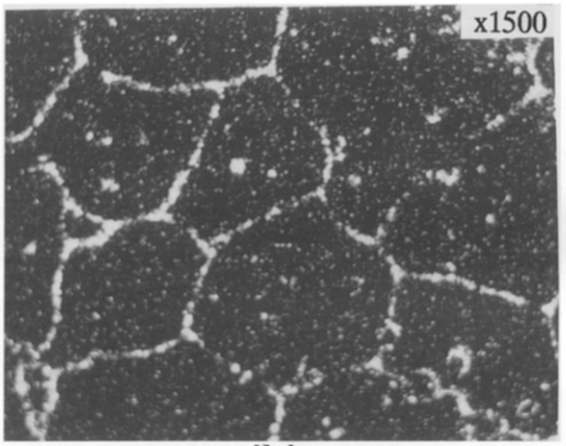

(b)

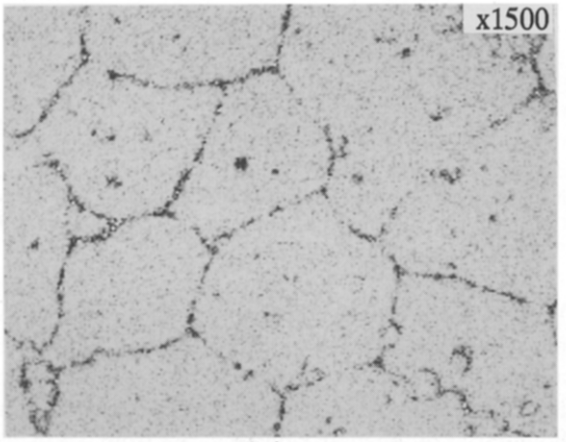

(c)

The fingerprint spectrum of yttrium $3d_{5/2}$ is overlapped by that of the bismuth $4f_{7/2}$, therefore the valence state of the yttrium ions could not be identified. However, it is well known that yttrium only has one oxidation state (Y^{3+}).

3.5. Transference number

Fig. 5 illustrates the ionic transference number (t_i) of $(Bi_{1.5}Y_{0.5}O_3)_{(100-x)\text{mol\%}}(Bi_2CuO_{4-0.5n})_{x\text{mol\%}}$ versus copper content at temperatures between 400 and 800°C. The t_i is reduced with increasing x, indicating that the second phase contributes to the electronic conduction. The t_i is independent of the oxygen partial pressure at the experimental range of $P_{O_2} = 1$ to 10^{-6} atm.

Ionic transference number (t_i) of $Bi_2CuO_{4-0.5n}$ at temperatures between 500 and 750°C are plotted in fig. 5. The t_i is almost zero when the temperature is below 700°C. When the temperature is above 700°C, t_i increases with increasing temperature. t_i is also independent of the oxygen partial pressures from $P_{O_2} = 1$ to 10^{-6} atm.

3.6. Electrical conductivity

The temperature dependence of the total conductivity for polycrystalline samples of $(Bi_{1.5}Y_{0.5}O_3)_{(100-x)\text{mol\%}}(Bi_2CuO_{4-5n})_{x\text{mol\%}}$ is plotted in fig. 6. Fig. 7 shows the total conductivity of $(Bi_{1.5}Y_{0.5}O_3)_{(100-x)\text{mol\%}}(Bi_2CuO_{4-0.5n})_{x\text{mol\%}}$ material as a function of oxygen partial pressure at various temperatures. Fig. 7 also shows the dependence of the oxygen partial pressure on the total conductivity for the synthesized $Bi_2CuO_{4-0.5n}$ material. The temperature dependence of the total conductivity for a polycrystalline sample of $Bi_2CuO_{4-0.5n}$ is plotted in fig. 8.

Fig. 1. Microstructure of the $(Bi_{1.5}Y_{0.5}O_3)_{95\text{ mol\%}}$ $(Bi_2CuO_{4-0.5n})_{5\text{ mol\%}}$ material. (a) Absorption electron image of the sample. (b) Copper X-ray mapping image. A copper-rich second phase is formed around the boundaries of the grains of the matrix phase. (c) Yttrium X-ray mapping image. A yttrium-rich matrix phase is surrounded by a copper-rich second phase.

Table 1
Chemical composition of the matrix phase in $(Bi_{1.5}Y_{0.5}O_3)_{90\ mol\%}$ $(Bi_2CuO_{4-0.5n})_{10\ mol\%}$ material obtained by WDS analysis.

Element	K (i_X/i_{std})	K (ratio)	Concentration (wt %)	Normalized Concentration (at %)
Y	0.3012	0.1028	10.837	9.879
Cu	0.0013	0.0011	0.088	0.19
Bi	0.7789	0.6705	77.396	30.00
O	0.13047	0.1231	9.357	59.97
Total		0.8975	97.677	100.03

Table 2
Chemical composition of the second phase in $(Bi_{1.5}Y_{0.5}O_3)_{90\ mol\%}$ $(Bi_2CuO_{4-0.5n})_{10\ mol\%}$ obtained by WDS analysis.

Element	K (i_X/i_{std})	K ratio	Concentration (wt %)	Normalized Concentration (at %)
Y	0.0046	0.0022	0.253	0.24
Bi	0.8043	0.6924	75.807	30.77
Ag	0.0000	0.0000	0.000	0.00
Ti	0.0000	0.0000	0.000	0.00
Cu	0.1473	0.1260	10.569	14.11
O	0.1453	0.1092	10.254	55.36
Total			97.052	100.48

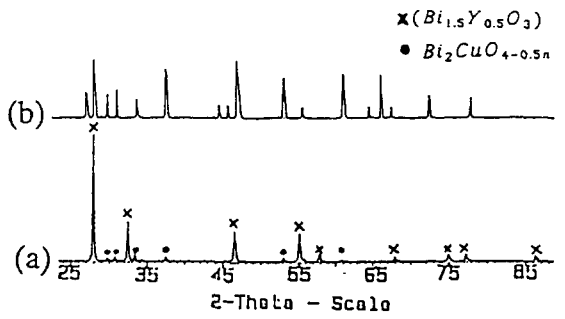

Fig. 2. XRD pattern of the (a) $(Bi_{1.5}Y_{0.5}O_3)_{90\ mol\%}$ $(Bi_2CuO_{4-0.5n})_{10\ mol\%}$ and (b) $Bi_2CuO_{4-0.5n}$ materials. The XRD is scanned at room temperature at a speed of 0.5°/min.

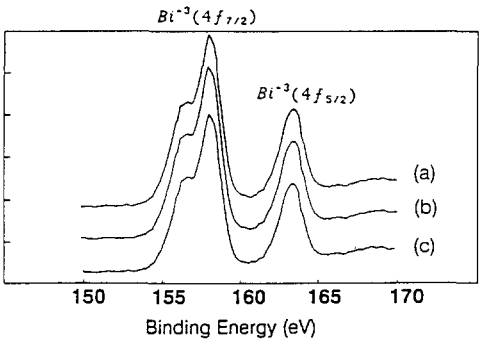

Fig. 3. XPS spectra of the 4f shell of bismuth measured under 10^{-9} Torr. (a) $(Bi_{1.5}Y_{0.5}O_3)_{90\ mol\%}$ $(Bi_2CuO_{4-0.5n})_{10\ mol\%}$ material measured at 750°C, (b) $(Bi_{1.5}Y_{0.5}O_3)_{90\ mol\%}$ $(Bi_2CuO_{4-0.5n})_{10\ mol\%}$ material measured at 25°C, and (c) $Bi_2CuO_{4-0.5n}$ material measured at 750°C.

4. Discussion

4.1. Microstructure

According to measured DTA data, when the sintering temperature is above 840°C, liquid $Bi_2CuO_{4-0.5n}$ phase will be formed in the materials. With well controlled liquid sintering, a continuous network second phase was formed even when the amount of the second phase was only 3 mol%. The thickness of the second phase formed around grain boundaries of the matrix phase varies from 0.5 to 20

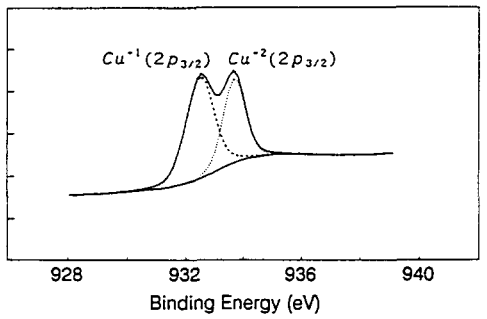

Fig. 4. XPS spectra of the 2p shell of the copper measured under 10^{-9} Torr at 750°C.

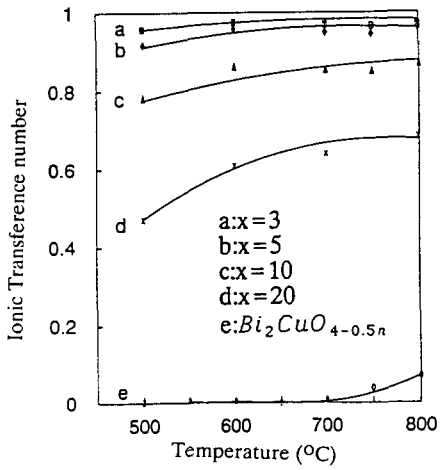

Fig. 5. Oxygen ionic transference number of the $(Bi_{1.5}Y_{0.5}O_3)_{(100-x)mol\%}$ $(Bi_2CuO_{4-0.5n})_{xmol\%}$ materials measured at temperatures between 500 and 800°C.

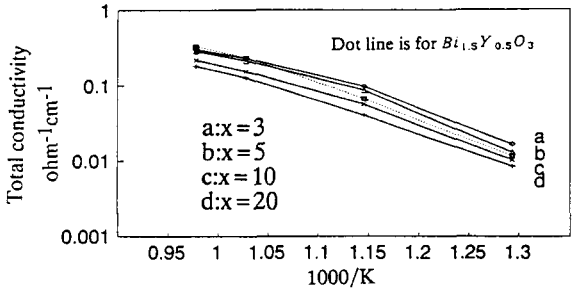

Fig. 6. Total conductivity versus temperature for $(Bi_{1.5}Y_{0.5}O_3)_{(100-x)mol\%}$ $(Bi_2CuO_{4-0.5n})_{xmol\%}$ materials measured in air.

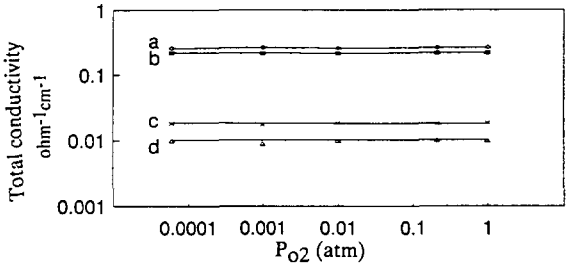

Fig. 7. Oxygen partial pressure dependence of the total conductivity at various temperatures. (a) $Bi_2CuO_{4-0.5n}$ material at 750°C, (b) $(Bi_{1.5}Y_{0.5}O_3)_{80\ mol\%}$ $(Bi_2CuO_{4-0.5n})_{20\ mol\%}$ material at 750°C, (c) $Bi_2CuO_{4-0.5n}$ material at 500°C and (d) $(Bi_{1.5}Y_{0.5}O_3)_{80\ mol\%}$ $(Bi_2CuO_{4-0.5n})_{20\ mol\%}$ material at 500°C.

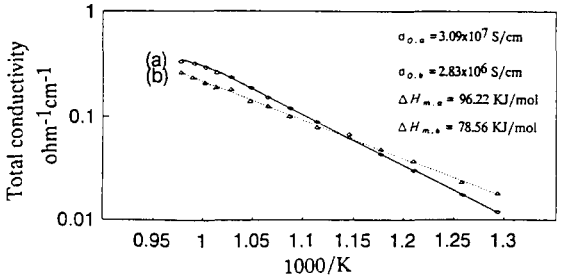

Fig. 8. Total conductivity versus temperature for: (a) $Bi_{1.5}Y_{0.5}O_3$ and (b) $Bi_2CuO_{4-0.5n}$ materials measured in air.

μm when the amount of the second phase increases from 3 to 50.

4.2. Crystal structure

The lattice parameter of the fcc matrix phase in $(Bi_{1.5}Y_{0.5}O_3)_{(100-x)mol\%}(Bi_2CuO_{4-0.5n})_{xmol\%}$ materials (5.5040 Å) is slightly smaller than that of $Bi_{1.5}Y_{0.5}O_3$ (5.5048 Å). The theoretical density of the matrix phase calculated according to measured lattice parameters is 8.30 g/cm^3. The calculated tetragonal lattice parameters of the second phase are $a=8.485$, Å, and $c=5.812$ Å, which are in agreement with the data reported ($a=8.484$ Å, $b=5.813$ Å) in ref. [8]. The parameters of the second phase are constant while the value of x changes from zero to 50. The theoretical density of $Bi_2CuO_{4-0.5n}$ according to the measured lattice parameters is 8.65 g/cm^3 for $n=0$, and 8.52 g/cm^3 for $n=1$.

4.3. Cation valence states

In 1971, Datta et al. [9] proposed an yttria-stabilized bismuth oxide formula of $Bi^{3+}_{3-x-y}Bi^{5+}_{x}Y_{1+y}O_{1+x}V_{0,(2-x)}$. In that paper, quantitative determination of pentavalent bismuth (Bi^{5+}) was not attempted due to lack of a straightforward method at that time. Harwig et al. [10] also proposed that the formation of Bi^{5+} or Bi^{4+} is possible in bismuth oxide from the viewpoint of the stability structure. As can be seen from the results of the XPS measurement in fig. 3, the binding energy of bismuth ($4f_{7/2}$) shows a single peak and keeps a constant value (158.5 eV) for both $Bi_2Y_{0.5}O_3$ and $Bi_2CuO_{4-0.5n}$. Therefore, this observation might rule out the possibility of significant Bi^{4+} or Bi^{5+} being present in the $Bi_2Y_{0.5}O_3$ or $Bi_2CuO_{4-0.5n}$ lattice.

For the first time in 1976, Arpe et al. [8] reported a Bi_2CuO_4 formula for the compound they found in the Bi–Cu–O system. However, the WDS measurement conducted by this study shows an oxygen-deficient formula of $Bi_2CuO_{4-0.5n}$. As can be seen in fig. 4, a binding energy of 932.4 eV corresponding to Cu^+ and a binding energy of 933.8 corresponding to Cu^{2+} are observed. The intensities of the two peaks are almost the same, implying that the mole ratio of the Cu^+ to Cu^{2+} is close to unity. With the combination of the chemical composition data obtained by WDS and the valence state data measured by XPS, a formula of $Bi_2Cu^{2+}_{1-n}Cu^{+}_{n}O_{0,(4-0.5n)}$ has been proposed for the compound found in the Bi–Cu–O system, and the n is about 0.5. The role of the multivalent copper cations in material's electronic conductivity will be addressed elsewhere [11].

4.4. Copper solubility in the matrix phase

A copper content, Cu/(Cu+Bi+Y), in the matrix phase of 0.5 mol% was measured by WDS microprobe in this study. Further evidence of soluble copper in the matrix phase was observed from the XRD measurement. The lattice parameter of the matrix phase was slightly smaller than that of the undoped $Bi_{1.5}Y_{0.5}O_3$ material, indicating that bismuth or yttrium ions may have been partially replaced by copper since the radius of Cu^{2+} (0.72 Å) is smaller than that of Y^{3+} (0.89 Å) and Bi^{3+} (0.96 Å) [12]. The lattice parameter is constant when x changes from 1 to 50, implying that copper is already saturated. At this point, it can be concluded that the solubility of the copper is very limited, and must be around 0.5 mol% or less.

4.5. Electrical properties of the matrix phase

To see the effect of the small amount copper on the electrical properties of the $Bi_{1.5}Y_{0.5}O_3$ matrix phase, a $(Bi_{1.5}Y_{0.5}O_3)_{99.5\ mol\%}$ $(CuO)_{0.5\ mol\%}$ material was fabricated and tested for its conductivity and transference number. The measured electrical properties of the $(Bi_{1.5}Y_{0.5}O_3)_{99.5\ mol\%}$ $(CuO)_{0.5\ mol\%}$ are almost identical to those of $Bi_{1.5}Y_{0.5}O_3$. Therefore, it can be concluded that the effect of 0.5 mol% copper on the electrical properties of $Bi_{1.5}Y_{0.5}O_3$ is negligible.

4.6. The electrical properties of the second phase

From the results of the transference number measurement (see fig. 5), it can be seen that the ionic conductivity of the $Bi_2Cu^{2+}_{1-n}Cu^{+}_{n}O_{4-0.5n}$ material is insignificant at temperatures below 700°C. The value of t_i increased from 0.034 to 0.067 when the temperature was above 700°C. Nevertheless, the oxygen ion conduction was still low even at high temperatures. In fig. 8, the total conductivities of the $Bi_2Cu^{2+}_{1-n}Cu^{+}_{n}O_{4-0.5n}$ and $Bi_{1.5}Y_{.5}O_3$ materials are plotted together for comparison. Listed in fig. 8 are the activation energy ΔH_m and pre-exponential term σ_0 of the conductivity for both $Bi_2Cu^{2+}_{1-n}Cu^{+}_{n}O_{4-0.5n}$ and $Bi_{1.5}Y_{.5}O_3$ calculated according to:

$$\sigma_{\text{total}}T=\sigma_0\exp\left(-\frac{\Delta H_m}{RT}\right). \quad (2)$$

4.7. Electrical properties of the composites

4.7.1. Parallel layer model

Assuming both phases are continuous, a parallel layer model can be used to calculate the total conductivity of the composite materials:

$$\sigma_{\text{total}}=(\sigma_{Bi1.5Y0.5O3})(1-V)+(\sigma_{Bi2CuO4-0.5n})(V), \quad (3)$$

where V is the vol% of the second phase. The ionic

conductivity and electronic conductivity of the composites calculated by the transference number and the parallel layer model, respectively, are listed in table 3. The electronic conductivities of the composites obtained by two methods match each other, confirming that the second phase is a continuous network phase.

4.7.2. Ionic partial blocking

The ionic conductivity obtained by the transference number, however, is smaller than that obtained by the parallel layer model. This is due to the fact that the continuity of the matrix phase is partially blocked by the surrounding second phase. To interpret the ionic partial blocked ionic conductivity, a modified parallel layer model is then expressed as:

$$\sigma_{\text{total}} = (F_b)\,(\sigma_{Bi_{1.5}Y_{0.5}O_3})(1-V) + (\sigma_{Bi_2CuO_{4-n}})(V)\,, \quad (4)$$

where F_b is an ionic partial block factor. Theoretically, F_b can be obtained by examination of the microstructure. However, it can be easily obtained by applying the modified parallel layer model to the ionic conductivity obtained according to the transference number. The value of F_b is given in table 3 as a function of the second phase and temperature. It can be seen that F_b decreases with increasing second phase.

4.8. Relation among transference number, temperature, and second phase

The conductivities for $Bi_{1.5}Y_{0.5}O_3$ and $Bi_2CuO_{4-0.5n}$ are equal at about 650°C (fig. 8). In

Table 3
Electrical properties of the $(Bi_{1.5}Y_{0.5}O_3)_{(100-x)\text{mol}\%}(Bi_2CuO_{4-0.5n})_{x\text{mol}\%}$ materials.

X (mol%)	T (°C)	σ_{total} (S/cm)	σ_{ion} [a] (S/cm)	σ_e [a] (S/cm)	σ_{ion} [b] (S/cm)	σ_e [b] (S/cm)	F_b
0	750	0.330	0.330	–	0.330	–	–
0	700	0.234	0.234	–	0.234	–	–
0	600	0.068	0.068	–	0.068	–	–
0	500	0.012	0.012	–	0.012	–	–
3	750	0.303	0.292	1.04×10^{-2}	0.317	1.06×10^{-2}	0.92
3	700	0.230	0.223	7.22×10^{-3}	0.225	7.27×10^{-3}	0.99
3	600	0.100	0.097	2.58×10^{-3}	0.065	2.57×10^{-3}	1.45
3	500	0.017	0.016	7.23×10^{-4}	0.011	7.20×10^{-4}	1.45
5	750	0.286	0.270	1.52×10^{-2}	0.312	1.58×10^{-2}	0.87
5	700	0.213	0.202	1.03×10^{-2}	0.220	1.09×10^{-2}	0.92
5	600	0.088	0.084	3.87×10^{-3}	0.064	3.85×10^{-3}	1.30
5	500	0.013	0.012	1.05×10^{-3}	0.011	1.08×10^{-3}	1.09
10	750	0.218	0.185	3.42×10^{-2}	0.289	3.30×10^{-2}	0.64
10	700	0.154	0.131	2.30×10^{-3}	0.205	2.27×10^{-3}	0.64
10	600	0.057	0.049	8.04×10^{-3}	0.060	8.03×10^{-3}	0.82
10	500	0.010	0.008	2.22×10^{-3}	0.010	2.25×10^{-3}	0.80
20	750	0.181	0.135	6.62×10^{-2}	0.248	6.60×10^{-2}	0.544
20	700	0.126	0.095	4.54×10^{-2}	0.176	4.55×10^{-2}	0.540
20	600	0.041	0.030	1.60×10^{-2}	0.051	1.61×10^{-2}	0.590
20	500	0.009	0.005	4.51×10^{-3}	0.009	4.50×10^{-3}	0.550
100	750	0.264	8.98×10^{-3}	0.255	8.98×10^{-3}	0.255	–
100	700	0.182	1.09×10^{-3}	0.178	1.09×10^{-3}	0.178	–
100	600	0.642	–	0.642	–	0.642	–
100	500	0.018	–	0.018	–	0.018	–

[a] Calculated using transference number.
[b] Calculated using parallel layer model.

accordance with the behavior of conductivity versus temperature, the ionic transference number of all $(Bi_{1.5}Y_{0.5}O_{0.5})_{1-x\text{vol}\%}(Bi_2CuO_{4-0.5n})_{x\text{vol}\%}$ materials increases with increasing temperatures. Owing to the ionic partial blocking factor, a $(Bi_{1.5}Y_{0.5}O_{0.5})_{65\text{vol}\%}(Bi_2CuO_{4-0.5n})_{35\text{vol}\%}$ composite material having about 30 vol% second phase, instead of 50 vol%, has a 0.5 ionic transference number at 650°C. Above 650°C the ionic transference number of $(Bi_{1.5}Y_{0.5}O_{0.5})_{65\text{vol}\%}(Bi_2CuO_{4-0.5n})_{35\text{vol}\%}$ is higher than 0.5, whereas below 650°C its ionic transference number is less than 0.5.

4.9. Relation between total conductivity and second phase

4.9.1. Case I. Second phase < 10 mol%

When the amount of second phase is small, the effect of the ionic partial block can be almost ignored. At high temperatures, the conductivity of the second phase is lower than that of the matrix phase. Therefore, the total conductivity of the composite material is smaller than that of the $Bi_{1.5}Y_{0.5}O_3$ single-phase material. At lower temperatures, such as below 650°C, however, the conductivity of the second phase is higher than that of the matrix phase. Consequently, the total conductivity of the composite material is higher than that of the $Bi_{1.5}Y_{0.5}O_3$ single-phase material.

4.9.2. Case II. Second phase > 10 mol%

When the amount of the second phase is more than 10 mol%, F_b rapidly decreases with increasing amount of second phase. As a consequence, the ionic conductivity as well as the total conductivity is dramatically reduced due to the ionic partial block effect. Even at temperatures below 650°C, the increasing conductivity contributed from the second phase cannot compensate the reducing conductivity due to the effect of the ionic partial block. Therefore, in the entire experimental temperature range, the total conductivity of the composite materials having more than 10 mol% second phase is smaller than that of the $Bi_{1.5}Y_{0.5}O_3$ single-phase material.

Theoretically, the composite material can be made with a high value of x to enhance the electronic conductivity. However, a composite material with a second phase higher than 25 vol% may not be practically useful due to its heavily blocked, low ionic conductivity.

5. Conclusions

A mixed ionic–electronic conductor consisting of a stabilized fcc $Bi_{1.5}Y_{0.5}O_3$ ionic-conductive matrix phase, and a tetragonal $Bi_2Cu^{2+}_{1-n}Cu^{1+}_nO_{4-0.5n}$ electronic-conductive second phase has been developed. The conductivity of the second phase is lower than that of the matrix phase at temperatures below 650°C, and is higher than that of the matrix phase at temperatures above 650°C. The network second phase, which is formed through the liquid-phase sintering at the grain boundaries of the matrix phase, contributes the electronic conduction. The matrix phase, the ionic conductivity of which is partially blocked by the second phase, contributes the ionic conduction. The ionic transference number is comparable with the electronic transference number at 650°C when about 30 vol% second phase is formed in the composite material.

Acknowledgements

The authors would like to thank Gas Research Institute for financial support under contract number 5090-260-1985. This research was conducted at Ceramatec Inc.

References

[1] M. Liu, A. Joshi, Y. Shen and K. Krist, Novel mixed ionic–electronic conductors for oxygen separation and electrocatalysis, US Patent No. 5, 273, 629 (1993).
[2] Y. Shen, M. Liu, A. Joshi and K. Krist, Solid State Ionics, submitted for publication.
[3] J.S. Subramanian, S.A. Akbar and K.S. Goto, J. Electrochem. Soc. 139 (1992) 2562.
[4] M. Liu, Y. Shen, A. Joshi and K. Krist, Mixed ionic and electronic conducting composite ceramic materials based on bismuth oxide and method of fabrication, US Patent Application serial No. 08/146, 880, filed on Nov. 1 (1993).
[5] Y. Shen, Ph.D. Dissertation (University of Utah, December 1993).
[6] C. Wagner, Z. Phys. Chem. 21 (1925) 25.
[7] T. Takahashi, H. Iwahara and T. Arao, J. Appl. Electrochem. 5 (1975) 187.

[8] V.R. Arpe and H.M. Buschbaum, Z. Anorg. Allg. Chem. 426 (1976) 1.
[9] R.K. Datta and J.P. Meehan, Z. Anorg. Allg. Chem. 383 (1971) 328.
[10] H.A. Harwig and J.W. Weenk, Z. Anorg. Allg. Chem. 444 (1978) 167.
[11] Y. Shen and A. Joshi, Structure and Transport Properties in Bi-Cu-O System, manuscript in preparation.
[12] R.D. Shannon and C.T. Prewitt, Acta. Crystallogr. B 25 (1969) 925.